AIAA JOURNAL
Vol. 47, No. 6, June 2009

Geometry Parameterization Method for Multidisciplinary Applications

W. Kyle Anderson,* Steve L. Karman,† and Chad Burdyshaw‡
University of Tennessee at Chattanooga, Chattanooga, Tennessee 37403

DOI: 10.2514/1.41101

A technique is described for parameterizing geometries in a manner suitable for numerical simulations used in design optimization. The new methodology, referred to as "control grids," is flexible, easy to use, extendable, and applicable to multidisciplinary design optimization. Although significantly different than free-form deformation, the present method provides many similar capabilities. Comparisons between the current technique and free-form deformation are provided to highlight the advantages and disadvantages of each method. The new parameterization technology is described and demonstrated in both two and three dimensions for single and multidisciplinary applications.

I. Introduction

THE use of numerical simulations for analyzing existing geometries is now routinely used in many industries. The simulations are also often used to conduct tradeoff studies for evaluating options that may lead to improved performance. In recent years, numerous researchers have been developing formal methods of determining sensitivity derivatives that can be used in conjunction with numerical optimization techniques to systematically reduce one or more cost functions that will subsequently lead to better performance of the vehicle in question [1–11]. For applications in which the shape is allowed to change to achieve the desired performance, it is necessary to describe either the geometry, or changes to the geometry, in terms of a set of parameters that are used as design variables to drive the optimization procedure. Example methodologies that have been used include the use of the individual mesh points on the surface of the mesh [3,6,12], Bezier, B-spline, and nonuniform rational B-spline (NURBS) surfaces [8,13–15], Hicks–Henne functions [1], sine functions [4], discipline specific functions [16], basis vectors [17], and free-form deformation [18–20]. A summary of some of the more prevalent parameterization techniques is given in [15]. Of particular interest is the method of free-form deformation (FFD), because it provides a convenient method for multidisciplinary design optimization applications in which it may be necessary to modify several unrelated meshes simultaneously. The FFD method uses a three-dimensional mesh in which each node in the mesh is considered to be a control point of a NURBS volume. The positions of the nodes are used as the design variables so that, as the control points are repositioned during the design process, the NURBS volume is reevaluated to provide changes to the original geometry. Although effective, in the most general implementation the number of design variables can be large if the mesh of control points is fully three dimensional. This is due to the fact that the number of nodes in the mesh increases as the cube of the number of points placed along the edges of the mesh. In [19], a methodology is described that alleviates the cubic dependence on the number of design variables to a quadratic dependence by replacing a trivariate FFD volume with a bivariate FFD surface that is placed onto the surface of the geometry.

In the present work, a technique for parameterizing geometries is described that has many of the advantageous features of FFD. However, in the current approach, the total number of design variables is not forced to grow cubically because design variables are typically distributed only on the surface of a control grid and do not require corresponding points to be distributed within the volume. Furthermore, the present technique uses a grid that remains fixed throughout the design process. This is in contrast to the FFD technique in which the control points are continuously moved and can potentially become tangled.

In developing the present technique, the following requirements are considered: 1) the methodology should be fast and easy to use, 2) it should be applicable to multidisciplinary design optimization, 3) it should be extendable to new situations as they arise, 4) it should produce smooth geometries, 5) it should allow for both small and large deformations, 6) it should not require a significant number of design variables, 7) it may be applied to large or small regions of the geometry to be designed, 8) it should provide a reasonably easy application of side constraints, and 9) accurate sensitivity derivatives should be readily obtained.

II. Control Grids

Although control grids may be used for both two- and three-dimensional applications, their use for parameterization is most easily described by initially considering a two-dimensional example. Figure 1 depicts an airfoil that is to be parameterized, along with an exemplary control grid surrounding the airfoil. To easily identify the geometry in the figure, the airfoil is depicted as a line, although in the present context it is actually composed of a series of discrete mesh points defining the surface. These mesh points are typically part of a larger-volume mesh. To use the control grid to modify the shape of the geometry, a set of partial differential equations with appropriate boundary conditions is discretized and solved on the control grid. The solutions of the discrete set of equations are considered as perturbations to the original surface and are interpolated and added to the points defining the original geometry. For use in shape optimization algorithms, the design variables stem from the boundary conditions associated with the partial differential equation.

Note that control grids provide a methodology for repositioning individual points, which may or may not be associated with a computational mesh. Although the methodology is presently applied to directly parameterize coordinates of a surface mesh, the technique

Presented as Paper 6028 at the 12th AIAA/ISSMO Multidisciplinary Analysis and Optimization, Victoria, British Columbia, Canada, 10–12 September 2008; received 18 September 2008; revision received 2 March 2009; accepted for publication 2 March 2009.

*Professor, SimCenter: National Center for Computational Engineering, 701 East M. L. King Boulevard. Associate Fellow AIAA.

†Research Professor, SimCenter: National Center for Computational Engineering, 701 East M. L. King Boulevard. Associate Fellow AIAA.

‡Assistant Research Professor, SimCenter: National Center for Computational Engineering, 701 East M. L. King Boulevard.

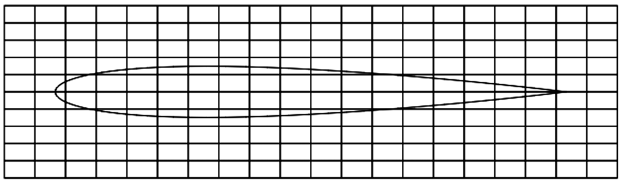

Fig. 1 Control grid surrounding an airfoil.

may also be applied to an environment in which the geometry may be defined using an underlying B-spline, NURBS, or similar representation. In this context, the control grid is used for modifying the positions of the control points associated with the spline, thereby modifying the geometry definition. In this manner, the method is not restricted to simply parameterizing mesh coordinates and can also be used in conjunction with other techniques, such as free-form deformation.

As a specific example, it is noted that a requirement specified earlier is that perturbations to the geometry be generally smooth. In this way, an initially smooth geometry will remain smooth after perturbations are added. This leads one to consider the use of elliptic partial differential equations, such as a Laplace-type equation, for each perturbation direction or equations for linear elasticity. In the present work, an approximation of Laplace's equation is solved for the perturbations p, q, and r in each of the x, y, and z directions, respectively:

$$\nabla^2 p = 0 \tag{1a}$$

$$\nabla^2 q = 0 \tag{1b}$$

$$\nabla^2 r = 0 \tag{1c}$$

The equations are discretized using commonly used finite difference formulas, although crude approximations to solving Laplace's equation have also been used, such as replacing the unknown at the central point in the stencil using simple averaging or inverse-distance weighting of the surrounding points. In each case, similar results are obtained in that the final designs are all virtually indistinguishable. Note that with the present implementation the perturbations added to the original geometry will not necessarily have smooth second derivatives, particularly on coarse control grids. The resulting geometry may not be smooth, which could manifest itself in the appearance of small oscillations in the pressure distributions, particularly for transonic flows. To achieve smooth second derivatives, both a higher-order solution method and a higher-order interpolation should be used. However, experience has shown that the higher-order approach is not required and that an easy and inexpensive way to circumvent this problem is to simply use a control grid that has spacing comparable to the spacing on the surface of the geometry. An example will be shown in Sec. III.

Dirichlet boundary conditions are used at the external boundaries of the control grid, although internal boundaries may also be considered, as described later in this section. Separate boundary conditions are applied to individual points on the boundaries of the control grid, and it is the magnitudes of the boundary conditions that become the design variables used to modify the shape. The boundary conditions for each of Eqs. (1a–1c) are set by first specifying a direction at each surface point that is either normal to the control grid, tangent to the control grid, normal to the surface of the geometry, or in an otherwise prespecified direction. A single magnitude is then used at each point so that the boundary values for each equation are determined by multiplying this magnitude by the relevant direction. Although the design variables are composed of the set of all the aforementioned magnitudes, the individual Cartesian perturbations, or even the directions of the perturbations, could be used as design variables. However, using a single magnitude for the perturbation reduces the number of design variables and allows for easier control in many cases. For example, if one wishes to control the thickness of a geometry that is not aligned with a coordinate axis, the control grid would be aligned with the geometry and perturbations normal to the upper and lower boundaries of the control grid could be obtained.

The solution of the discretized equations is obtained with a simple point-iterative procedure using a fixed number of iterations. The solution of these equations accounts for almost all the computational work in the process, as it needs to be repeated once for each design variable. However, because a linear partial differential equation is used and the perturbations are always added to the original geometry, these solutions only need to be done once and the results saved in a table. Although the equations need to be solved for every design variable, it is important to note that it is not necessary to obtain a highly converged solution, as the purpose of the entire process is simply to propagate perturbations from the boundaries into the interior. Typically, the solution process is stopped after only a few orders of magnitude of convergence and experiments have indicated that there is no benefit to obtaining a highly converged solution. After the solutions to Eqs. (1a–1c) are obtained, the coordinates of each mesh point may be updated by adding the associated perturbations:

$$x^{\text{new}} = x^{\text{original}} + p \tag{2a}$$

$$y^{\text{new}} = y^{\text{original}} + q \tag{2b}$$

$$z^{\text{new}} = z^{\text{original}} + r \tag{2c}$$

With the aforementioned smoothing procedure, the number of design variables is proportional to the number of mesh points lying on the boundaries of the control grid. A reduction in the number of design variables can be obtained by specifying a coarser distribution on the surface of the control grid at locations that may not coincide with the actual points in the control grid. The boundary values at the points on the surface of the control grid are then obtained by interpolation. In the present implementation, this is achieved by defining a "design grid," which is coarser than the control grid but has the same general shape. The design variables are associated with points lying on the boundaries of the design grid, and the boundary conditions for the control grid are obtained by interpolation. An example is given in Fig. 2 for a two-dimensional control grid. Here, the design grid consists of a series of points defined on each boundary of the control grid. Note that the number of points on each boundary is not required to be the same. Furthermore, in some applications it may be advantageous to define boundary conditions that are applied to larger regions of the control grid. A natural example would be specifying a single boundary condition that is applied around the entire perimeter of an axisymmetric control grid.

In three-dimensional applications, a similar procedure may be followed in which the boundary values on the surface of the control grid are obtained using bilinear interpolation of the design variables from the design grid and are then propagated into the interior using Laplace's equation. However, other variations are available in three dimensions that provide extended capabilities. For example, instead of using bilinear interpolation on a surface face of a hexahedral control grid, design variables may be transferred from the design grid to the control grid by first using linear interpolation only along the four perimeter edges of the face to determine the boundary

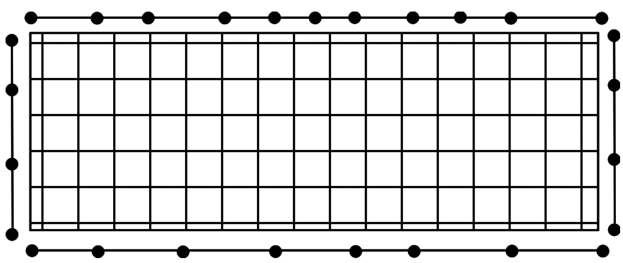

Fig. 2 Control grid including the depiction of points on the design grid surface.

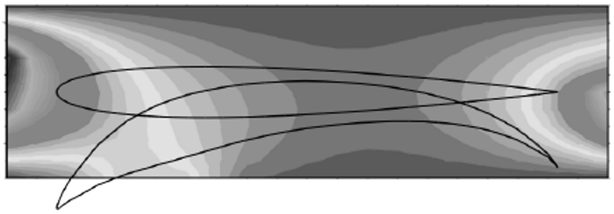

Fig. 3 Example deformations in the *y* direction using the control grid.

conditions for the control grid along these edges. A "two-dimensional" smoothing procedure is then used within each surface face to obtain the variables at the remaining points within the face. This procedure may be used on one or more surfaces of the control grid, with the values on the remaining faces determined using bilinear interpolation. This procedure is referred to here as "face smoothing."

An example of using a control grid to manipulate a geometry is shown in Fig. 3. In this example, the initial geometry corresponds to a NACA 0012 airfoil, which is placed approximately in the center of the control grid. The smoothing procedure is applied in each direction independently, and the boundary conditions are specified so that perturbations are only allowed in the vertical direction, thereby eliminating the need to solve for perturbations in the horizontal direction. As seen in the figure, the new airfoil geometry is greatly modified from the original and the contours of the perturbations appear to be smooth. Note also from the figure that the modified geometry extends beyond the boundaries of the control grid. Because the perturbations are relative to the original geometry and because the control grid is fixed, large deformations can be obtained with no tangling of the control grid, which could happen with free-form deformation. Note, however, that although the control grid cannot become tangled, the geometry itself could cross. For example, if large positive vertical perturbations are specified on the lower portion of the control grid and large negative perturbations are specified on the upper portion of the control grid, it is possible that the lower and upper surfaces could cross. As with other methods, placing limits on the design variables can control this.

During the design process, mesh sensitivities are generally required as the geometry deformations at the surface are propagated into the interior. The means for propagating the boundary changes to the interior mesh points is not generally dependent on the parameterization of the surface and can be accomplished with many techniques [7,11,21–23]. However, the determination of mesh sensitivities inevitably requires the sensitivity derivatives of the surface mesh points with respect to the design variables. Because of the linearity of the present smoothing algorithm and because the geometry is always perturbed in relation to the original shape, the sensitivity derivatives of the surface points with respect to the design variables are easily obtained by sequentially setting each design variable to unity while setting the remainder of the boundary conditions to zero. After solving the equations, the solution corresponds to the sensitivity derivatives. Although this parameterization technique requires the solution of the perturbations for each design variable, the sensitivity derivatives of the surface points are fixed throughout the design process so that the solution of the perturbations is only required at the initial step and need not be repeated during each design cycle. Again, this is because of the linearity of the smoothing procedure and because the geometry is always modified in relation to the original geometry. This also facilitates determining bounds on design variables because the changes to the surface are proportional to the product of the sensitivity derivatives and the changes in the design variables, making it easy to examine the changes in the geometry with each change in a design variable. Finally, it should be recalled that a highly converged solution is not required, provided that the boundary conditions propagate into the interior.

To examine the ability of the current procedure to obtain general shapes while not producing high-frequency oscillations, a NACA 0012 airfoil is used as an initial geometry, and a target geometry is obtained by randomly moving points on the lower surface of the airfoil. A single control grid is used in which vertical perturbations are allowed on the top and bottom boundaries and zero perturbations are prescribed on the left and right sides of the control grid. The control grid has 201 points in the horizontal direction and 81 points in the vertical direction. There are 32 design variables evenly spaced on the upper and lower boundaries for a total of 64 design variables. Figure 4a depicts the original airfoil geometry, the current geometry, and the target geometry. The current geometry is obtained after 10 design cycles using a trust-region method [24], and the cost function is the squared difference between the coordinates of the current geometry and the target geometry. Figure 4b shows contours of the perturbations in the control grid as well as the final geometry. As seen in Fig. 4a, the present method reproduces the target geometry reasonably well, although it does not capture the higher-frequency oscillations near the leading edge. As with any method used to specify design variables, it may not be possible to obtain all target geometries as the perturbations only have a finite-dimensional basis and do not necessarily provide enough flexibility to account for arbitrary changes. Increasing the number of design variables or modifying the smoothing procedure to give greater weight to the vertical perturbations may capture this high-frequency oscillation.

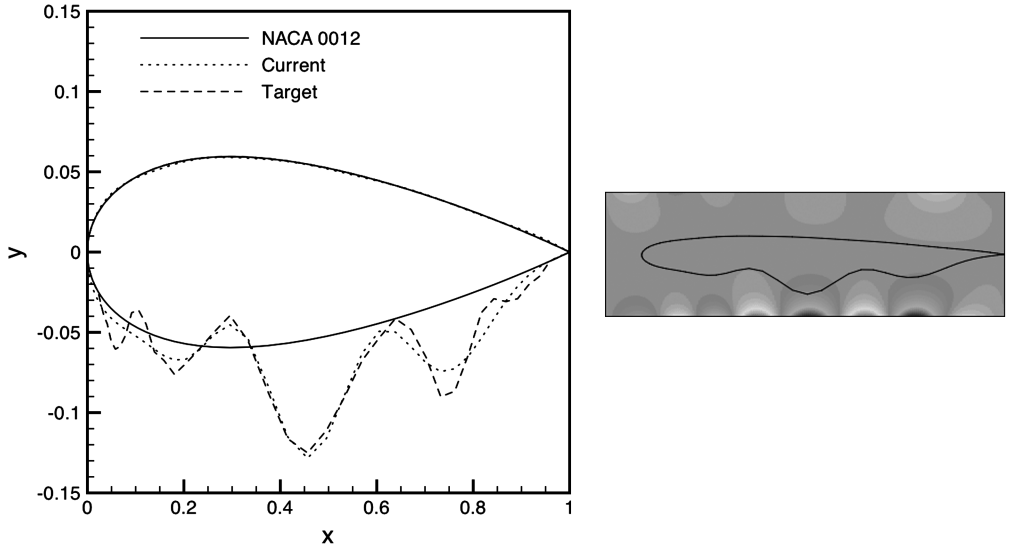

a) Geometry coordinates **b) Perturbations**

Fig. 4 Airfoil deformation.

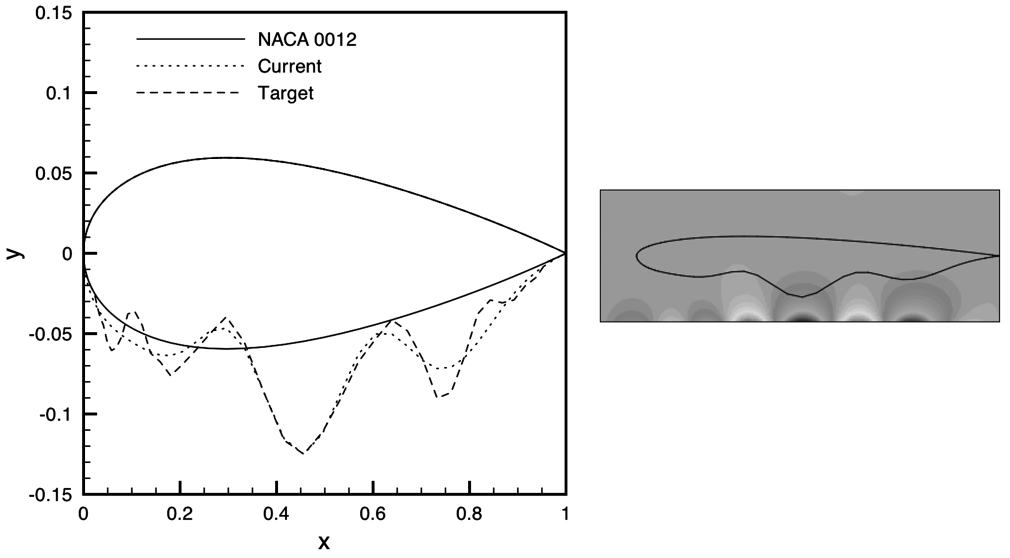

a) Geometry coordinates **b) Peturbations**

Fig. 5 Airfoil deformation with the upper surface held fixed.

Note that, from the contours depicted in Fig. 4b, the design variables successfully adjust to produce the oscillations on the lower surface while reasonably maintaining the original geometry on the upper surface. It should be noted that repeating this experiment using several control grids of varying extent in the vertical direction from 0.1 to 0.5 has very little effect on the final answer.

In the results shown in Fig. 4, the upper surface points have been approximately held fixed by explicitly including them in the cost function. With close examination, however, a very slight variation between the current geometry and the original geometry can be seen on the upper surface approximately 10% aft of the leading edge. A more direct way to hold the upper surface fixed is to simply place the control grid so that it only affects the geometry points on the lower surface of the airfoil. Although using this technique may be suitable in some instances, a more general procedure is to initially determine the points in the control grid that surround the constrained geometry points and then simply specify zero perturbations at those control points during the solution procedure. This method is easily automated and can be viewed as enforcing internal boundary conditions during the solution for the perturbations.

Figure 5 depicts results obtained using the internal boundary condition procedure for the same problem shown earlier in Fig. 4. As seen in Fig. 5a, the fidelity of the upper surface is successfully maintained whereas the lower surface is allowed to change. Further, from the contours of the perturbations shown in Fig. 5b, the perturbations appear to be smooth. However, it should be noted that the geometry at the interface between the fixed points and the points that are allowed to move may not be smooth, particularly if the perturbations at the adjoining points are large. This is because the fixed point is essentially a boundary between the stationary curve and the variable curve, with no present mechanism implemented for enforcing smooth second derivatives at the juncture.

There are many ways to incorporate control grids into the parameterization process. First, note that, although the aforementioned examples have all been based on rectangular structured meshes, there is no requirement that this be the case. For example, in two dimensions, the control grids may be circular, triangular, elliptical, or virtually any other shape that is convenient for the application and may use structured or unstructured indexing. Similarly, for three-dimensional applications, the control grids can be cubes, spheres, cylinders, pyramids, tetrahedra, or combinations of these, although these shapes are in no way inclusive. Control grids may be deployed such that they surround one or more geometries or even just portions of the geometries. However, a control grid surrounding a geometry will not necessarily modify that geometry unless that geometry is explicitly "associated" with the control grid. For example, in Fig. 6a, a single control grid surrounds both airfoil geometries. The perturbations obtained on the control grid may be interpolated to both geometries but may optionally only be used to modify the shape of one of them. In an alternate deployment shown in Fig. 6b, two control grids are associated with a single geometry. As also seen in Fig. 6b, the control grids may be used to modify large or small regions of any geometry being parameterized. For the example in Fig. 6b, the points lying outside the control grids would remain fixed, which could potentially lead to a lack of smoothness at the interface, as there is no technique presently implemented to enforce smooth second derivatives. Obtaining smooth transitions between these regions is more easily implemented in FFD by fixing several rows of control points in these areas. Note, however, that using control grids to manipulate control points of an underlying spline definition would also eliminate this problem. Multiple control grids may also be used to modify the same points on a given geometry. In this instance, the final perturbation that gets added to the original geometry is the sum of the perturbations from each control grid. Finally, it should be noted that algebraic changes, such as sweep or twist, may also be easily included through specification of the boundary conditions for the partial differential equations or by directly specifying these changes at individual points on either the control grid or the geometry itself.

Note that, for internal flows, a situation can occur using the present technique, which will be referred to as "blocking." Referring again to Fig. 6a, if the design variables are placed only at the external boundaries of the control grid, and the upper surface of the top airfoil and the lower surface of the bottom airfoil are held fixed using the internal boundary condition procedure described in reference to Fig. 5, the perturbations prescribed on the external boundaries could be prevented from propagating into the interior of the control grid. In most applications this is easily remedied by simply using a separate control grid for each geometry. In three-dimensional applications, it may be desirable to modify the internal surface of a geometry while holding the outer surface fixed. A typical example would include the design of the internal shape of an inlet while holding the outer mold lines of the nacelle fixed. Blocking may be alleviated using several techniques. The easiest method is to simply designate the interior surfaces as separate geometries that are then associated with a control

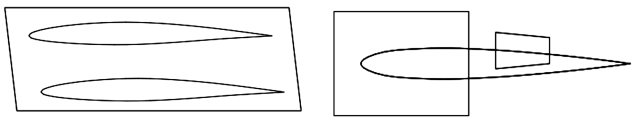

a) Single control grid around two geometries **b) Two control grid around single geometry**

Fig. 6 Example uses of control grids.

grid. Blocking can also be alleviated by ensuring that the control grid is finer than the defining points on the geometry so that the perturbations are allowed to propagate between the fixed points and into the interior of the control grid: although not shown, this approach has been successfully used. Alternatively, a control grid may be placed between the two surfaces so that only the interior surfaces will be modified. Other approaches would include using some of the points in the interior of the control grid as design variables, using Neumann boundary conditions, or devising a suitable control grid with a passage through it (for example, a hollow tube). In the latter case, design variables could be placed on the inner and outer surfaces of the tube. Source terms can also be used and may be implemented using a methodology similar to that described in [25], which prescribes source terms that are used in determining mesh spacing for an advancing-front grid generation algorithm.

III. Results

Results are given in this section for both two- and three-dimensional applications. In the two-dimensional applications, an unstructured Euler solver similar to that described in [26] is used to determine the variables in the flowfield, whereas sensitivity derivatives are obtained using the complex-variable method of forward-mode differentiation described in [27–29]. Although the examples are for inviscid flows, it should be noted that the parameterization method is only used to modify surface points and is thus applicable to viscous flows as well. For both two- and three-dimensional optimization cases, the computational mesh used for solving the governing equations (Euler or Navier–Stokes) is modified during the design cycles to reflect the evolving geometry by treating the mesh as a structure in which perturbations on the boundaries obtained using the control grids are propagated into the interior using assumptions of linear elasticity [11].

In the first example, the initial geometry is a NACA 0012 airfoil at a freestream Mach number of 0.5 and an angle of attack of 1.25 deg. The goal of the design is to increase the lift coefficient from its initial value of 0.17 to a target value of 1.0. For this test, two control grids are used and the design is repeated separately for each. In each case, the design variables on the upper and lower surfaces of the control grid provide perturbations in the vertical direction, whereas the design variables on the left and right sides of the control grid are held constant at zero. In the first control grid, shown in Fig. 7a, the leading edge of the airfoil is placed a specified distance from the left side of the control grid, whereas the trailing edge is placed adjacent to the right side of the control grid. Because the perturbations on the right-hand side of the control grid are zero, the effect of this placement is to allow the vertical position of the leading edge to change while the trailing edge is held fixed. Note that the trailing edge could also be held fixed using the internal boundary condition approach described earlier. The second control grid, depicted in Fig. 7b, is constructed so that the leading and trailing edges of the airfoil are both placed adjacent to the boundaries of the control grid, thereby effectively fixing those points.

After only two design cycles using a trust-region method [24], the final lift coefficient is successfully obtained for each case. As seen in Fig. 8a, the resulting pressure distributions show significant changes in comparison to that for the baseline NACA 0012. In addition, the pressure distributions for the modified geometries are each somewhat different, reflecting the effectively different constraints on the geometries. As seen in Fig. 8b, the modified geometries are similar to each other, although they are significantly different from the original. Furthermore, Fig. 8c shows a close-up of the leading-edge geometries and illustrates the differences obtained using the different parameterizations. In particular, when using the first control grid, the leading edge of the airfoil is slightly raised when compared with the other geometries.

The control grid used for these results has only 21 points in the streamwise direction and 11 points normal to the airfoil. As seen in the results, the pressure distribution is smooth. As mentioned earlier, this may not be achieved for transonic flows, which are more sensitive to variations in the surface. An example is shown in Fig. 9, which depicts results for a NACA 0012 at a Mach number of 0.8 and an angle of attack of 1.25 deg, for which the objective of the design is to reduce the drag coefficient while maintaining the lift. The initial pressure distribution, shown in Fig. 9a, is smooth away from the shock, with lift and drag coefficients of 0.3543 and 0.0229, respectively. Note that this solution, as with the solutions after modifying the shape, has not been obtained using a flux-limiting procedure and there are typical oscillations at the shock wave. Modified designs have been obtained using a coarse control grid of 21×11 and a fine control grid of 81×41. The number and placement of the design variables is the same in both cases, with 19 design variables evenly distributed along the lower surface of the control grid and 9 evenly distributed across the top. After five design

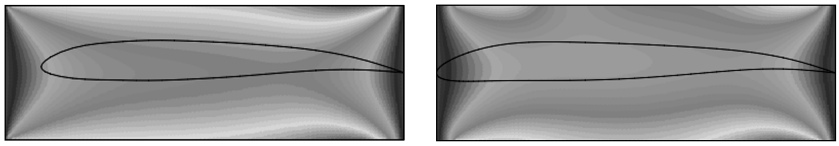

a) Floating leading edge **b) Fixed leading edge**

Fig. 7 Control grid boundaries and perturbations.

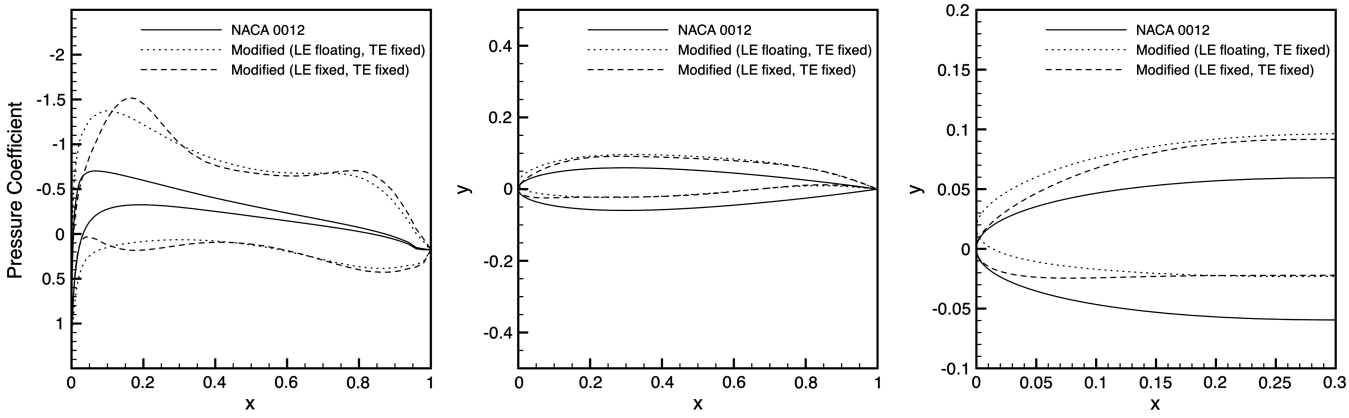

a) Pressure distributions **b) Geometries** **c) Geometries near leading edge**

Fig. 8 Redesigned airfoil.

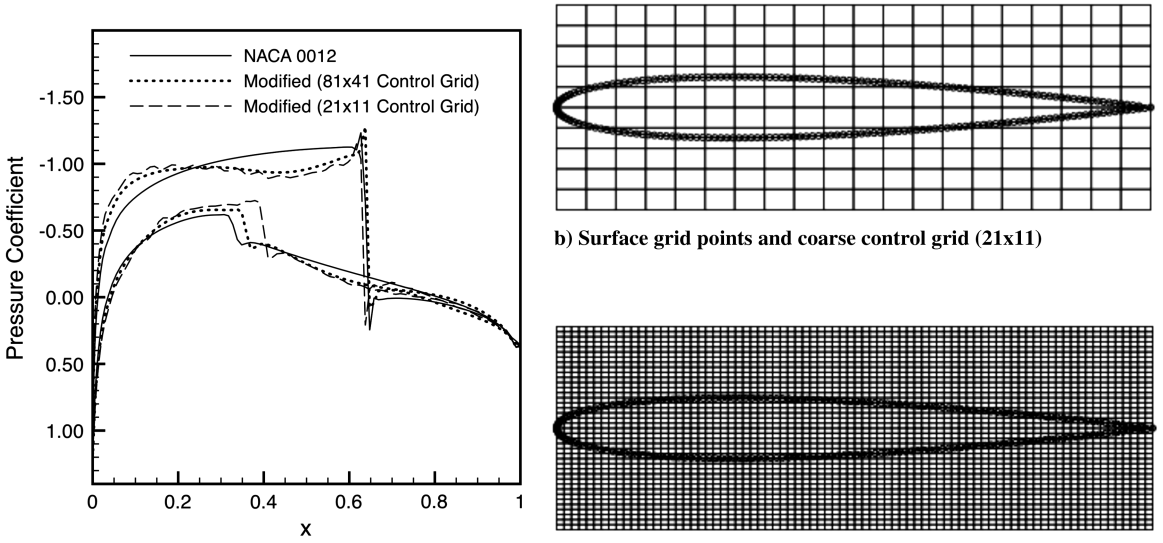

a) Pressure distributions

b) Surface grid points and coarse control grid (21x11)

c) Surface grid points and fine control grid (81x41)

Fig. 9 Effect of the control grid on the smoothness of pressure distribution for the transonic airfoil.

cycles using the finer control grid, the lift has dropped 2% whereas the drag is reduced 47%. Similar results are obtained using the coarser control grid with a 3% drop in the lift coefficient and a 58% reduction in drag. Note that, in both cases, the shock is not eliminated. This is due to the fact that small local variations in the surface, which can be very effective at eliminating shocks for single-point designs, are not generally obtained using the current method. As seen in Fig. 9a, the final pressure distribution after modification using the coarser control grid exhibits noticeable oscillations ahead of the shock whereas the pressure distribution obtained using the finer one remains smooth. Numerical experiments have shown that oscillations can generally be avoided, provided the control grid has similar spacing as the surface of the geometry.

The next demonstration case uses the parameters on a control grid as the design variables for changing the shape of an airfoil from a NACA 0012 to an RAE 2822 [30]. The freestream Mach number is fixed at 0.63, whereas the angle of attack is 2 deg. For this example, an initial solution has been obtained for the RAE 2822, which is interpolated onto the surface of the NACA 0012 and used as a target pressure distribution. There are 23 design variables evenly spaced along the upper and lower boundaries of the control grid, for a total of 46 design variables. After 15 design cycles, the objective function has been reduced from 0.0464 to 0.0008, and the rms gradient of the objective function with respect to the design variables has been reduced from 0.1280 to 0.0013. As seen in Figs. 10a and 10b, the target pressure distribution and target geometry are obtained reasonably well. Contours of the perturbations are shown in Fig. 10c along with the final shape and demonstrate the primary areas in which changes have occurred.

A final two-dimensional example is shown in Figs. 11 and 12 for a transonic slotted airfoil, originally described in [31]. For the case considered here, the Mach number and angle of attack are 0.7 and 1.0 deg, respectively. The cost function is defined as a linear combination of the lift and drag coefficients, so that the lift will remain approximately constant while simultaneously reducing the drag. The lift on the baseline configuration is 0.1359 with a corresponding drag coefficient of 0.0402. Figure 11a depicts the initial and final shapes of the main element and the flap, whereas Fig. 11b shows the control grid as well as the contours of vertical perturbations after the design. For this case, the control grid is not rectangular and contains 101 points in the direction approximately aligned with the freestream and 41 points in the normal direction. Only seven design variables are used on the top and bottom boundaries of the control grid, for a total of 14 design variables. As seen in Fig. 11b, the control grid extends ahead of and behind the airfoil. The trailing edge of each airfoil is held fixed by specifying internal boundary conditions, as described earlier.

After 10 design cycles, the final lift and drag coefficients are 0.1351 and 0.0222, respectively, resulting in a 40% decrease in drag coefficient. It is seen in Fig. 11a that the upper and lower surfaces of

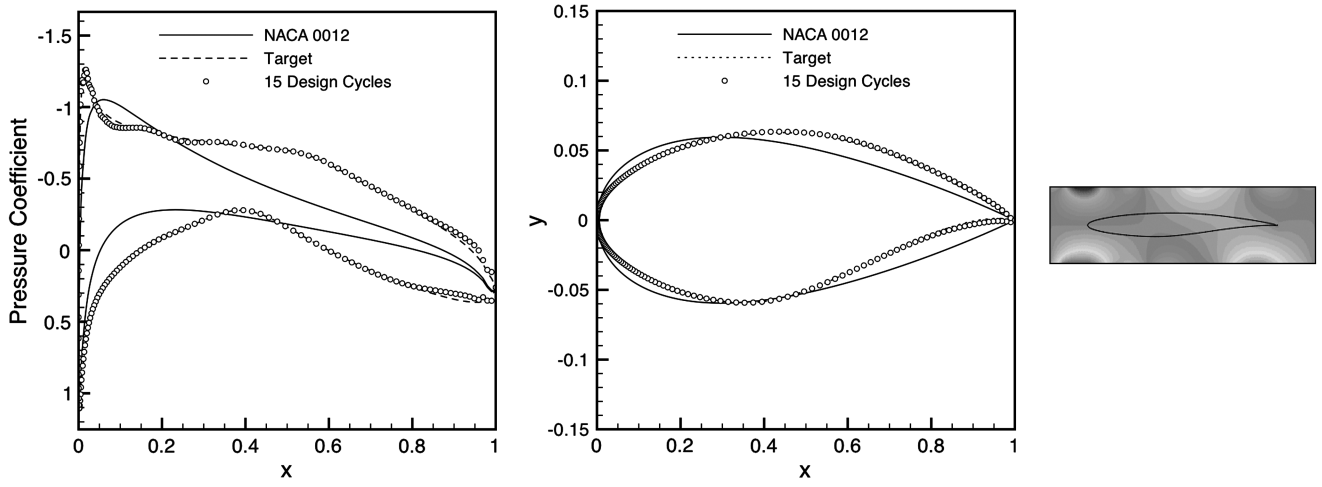

a) Pressure distributions

b) Geometries

c) Perturbations

Fig. 10 Comparison of the original and modified designs of the RAE 2822 airfoil.

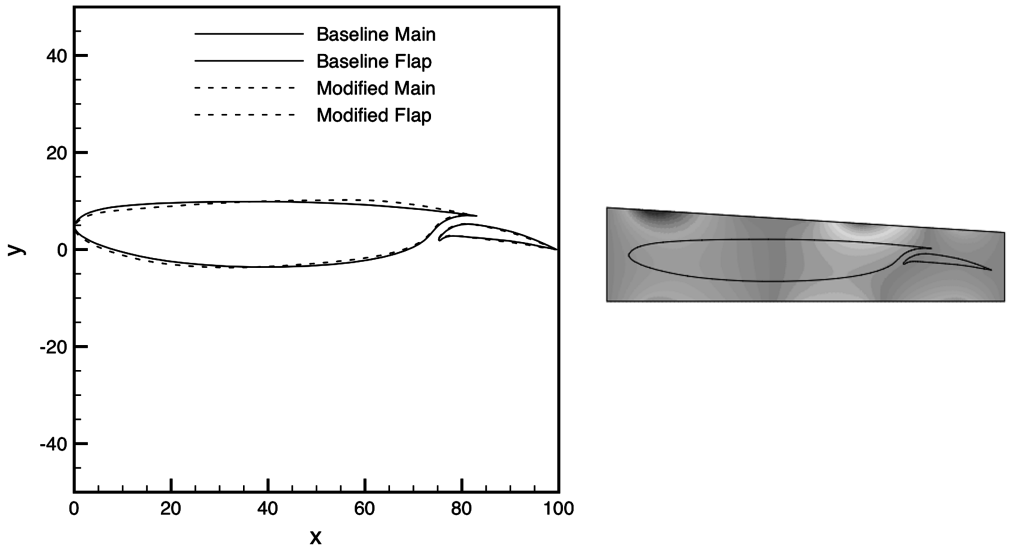

a) Baseline and modified geometries **b) Control grid perturbations**

Fig. 11 Two-element airfoil.

the modified airfoil near the leading edge of the main element are slightly lower than the baseline geometry, although the overall thickness is approximately unchanged. Toward the aft end of the main element, the upper surface is slightly above the original surface, whereas the lower surface is only very slightly raised. Consequently, the thickness at the aft end of the main element is increased. The geometry of the flap on the modified airfoil appears to be only slightly changed over that of the original geometry. Density contours for the baseline and modified geometries are shown in Figs. 12a and 12b, respectively. After the design, the shock on the main element is not eliminated but is smaller in extent when compared with the baseline configuration.

The control-grid methodology has also been developed and tested for three-dimensional applications. For these applications, the flow solver developed at the University of Tennessee at Chattanooga [32,33] is used for analysis of the flowfield, the adjoint solver as described in [34,35] is used to obtain the solution gradients, and the PORT trust-region optimization code is used [24].

To demonstrate the methodology in three dimensions, three examples are provided. For the first example, shown in Figs. 13 and 14, three compressor blades have been parameterized using a separate control grid for each blade. In this example, an optimization is not performed but forced changes are imposed to artificially manipulate the geometry. The initial geometry is shown in Fig. 13a,

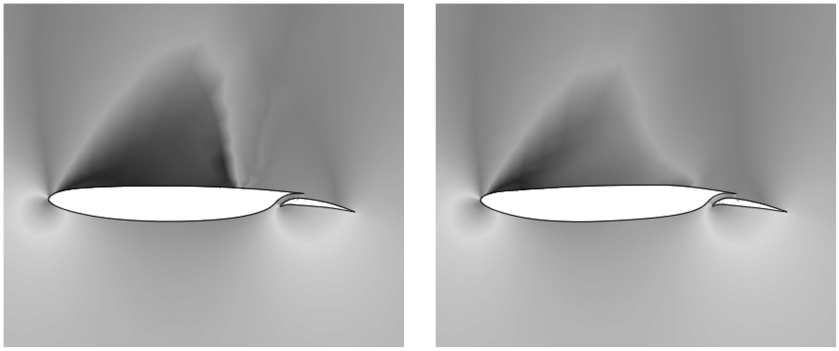

a) Density contours for baseline geometry **b) Density contours for modified geometry**

Fig. 12 Two-element airfoil.

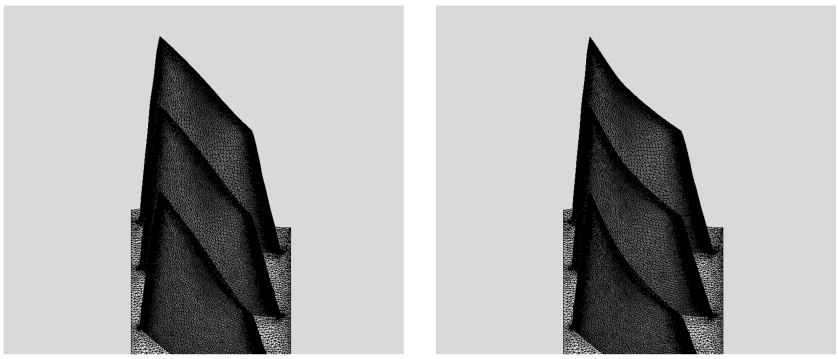

a) Baseline compressor blades **b) Modified compressor blades**

Fig. 13 Compressor blades.

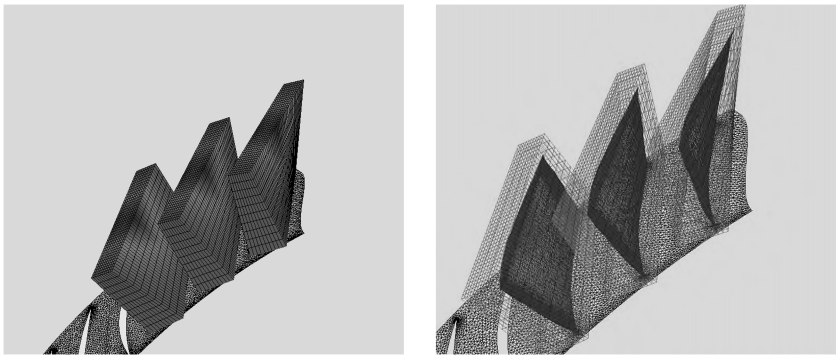

a) Control grids for compressor blades b) View of control grids surrounding each blade

Fig. 14 Control grids for compressor blades.

whereas the modified geometry is depicted in Fig. 13b. In each figure, the contours represent the magnitude of the perturbations. As seen, there are significant changes applied to the original shape. It should be noted that the control grids in this case, shown in Figs. 14a and 14b, are devised so that all the blades are parameterized with a single set of design variables, and that changes in these design variables effect all the blades in the same manner. It can also be seen from Fig. 14a that each control grid has a significant amount of twist, which reflects the underlying twist of the associated blades. Figure 14b demonstrates that the control grids for this case conform roughly to the angles of each of the blades. However, similar results have also been obtained using nontwisted control grids. Note also that, although the control grids shown in Fig. 14 do not overlap, significant overlap in the control grids is obtained using the nontwisted control grids. This does not adversely affect the procedure as each blade is separately assigned to a control grid.

Figures 15a and 15b depict the second three-dimensional example. Here, shape optimization is used to double the lift coefficient for a wing while holding the Mach number and angle of attack fixed at 0.6 and 3.0 deg, respectively. The initial geometry, shown in Fig. 15a, is an unswept wing with NACA 0012 airfoils at each spanwise station. Also shown in the figure is a representative structural model that includes several ribs and wing spars. The upper surface of the wing is shown to be transparent so that the structural model can be clearly seen, whereas the tip region is opaque to more clearly demonstrate the changes to the airfoil section near the tip. It should be noted that, although a structural model is shown, no structural analysis is actually included as part of the optimization procedure. As such, the structural model is "passive" and is only included to demonstrate that, although the aerodynamic and structural grids have been generated independently, they change simultaneously in response to changes in the design variables. As with Fig. 13, the contours indicate the size of the perturbations that are applied to the original geometry after the optimization.

The design grid for this case is $6 \times 6 \times 2$, with only two planes of design variables in the spanwise direction, and is shown in Fig. 16a.

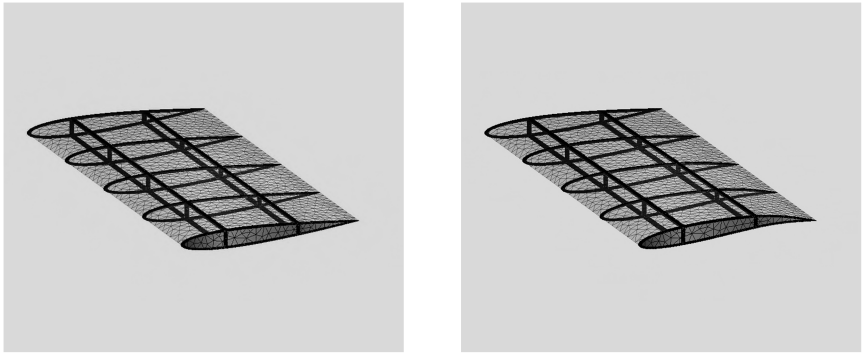

a) Initial geometry including internal structure b) Final geometry including internal structure

Fig. 15 Wing design for specified lift with floating structure.

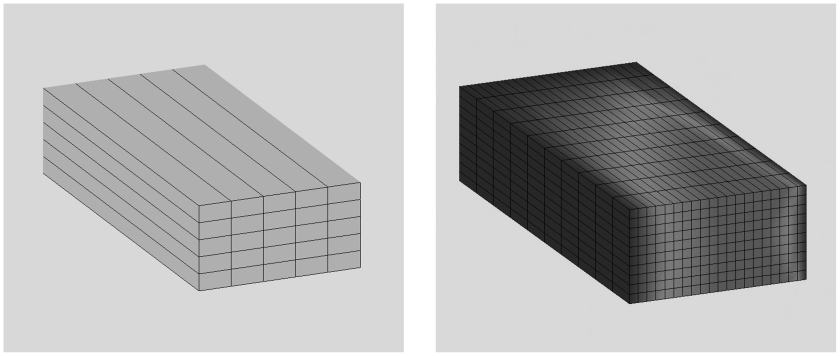

a) Design grid b) Control grid with perturbations

Fig. 16 Face smoothing grids.

The control grid, shown in Fig. 16b, has only 11 points in the spanwise direction with a 21×11 grid in the plane normal to the span. To transfer the design variables from the design grid to the control grid, face smoothing is used in the plane of the control grid nearest the wing tip, whereas the data on the remaining planes are determined using bilinear interpolation from the design grid. The entire volume is then smoothed to propagate the perturbations at the boundaries into the interior. In this application, the only nonzero design variables are those that lie on the upper and lower line segments defining the plane nearest the wing tip. Combined with the fact that only two spanwise planes are used for the design grid, the effect is that modifications are made to the geometry of the airfoil sections near the tip, which decrease linearly as the wing root is approached. In this manner, changes in the airfoil profiles may be introduced without the possibility of simultaneously causing spanwise oscillations, and so the airfoil sections vary smoothly between the wing tip and the root. As seen in Fig. 16b, after the optimization is complete, larger perturbations are evident on the face of the control grid nearest the tip, which subsequently decrease as the root is approached. Furthermore, it is noted that larger changes occur aft of the midchord, indicating that aft-cambered airfoil sections are created.

After only two design cycles, the target lift has been achieved to 11 decimal places. As shown in Fig. 15b, the final geometry exhibits noticeably more camber at the tip, which decreases linearly to zero at the wing root. As also observed, the structural model has been deformed in response to changes in the design variables and remains congruent with the aerodynamic model.

The final three-dimensional case is a low-Reynolds-number flow through a manifold, which roughly represents a generic geometry for a fuel-cell application. Referring to Fig. 17a, the flow enters the manifold at the lower-left corner, traverses through the channels, and exits at the upper-right corner of the geometry. As seen from the velocity contours in Fig. 17a, it is observed that the majority of the flow goes through the last channel, with a significant amount of flow also going through the first channel. Because the channels in the middle of the manifold have significantly less flow, in a fuel-cell application this could lead to inefficiencies due to the potential of starving the central channels of fuel. To improve the apportioning of flow among the channels, a control grid with seven design variables has been used on both the upper and lower walls for reshaping these regions. To keep the top and bottom surfaces planar, face smoothing is used on the front and rear faces, wherein the design variables on the rear face are copied onto the front face. This also reduces the number of design variables and demonstrates the flexibility for adapting the control grids for specific purposes. After five design cycles, the final geometry, shown in Fig. 17b, demonstrates significant curvature of both the upper and lower walls. It is evident from the contours that the mass flow is much better distributed across the channels. This is quantified in Fig. 18, which shows the mass flow in each channel for the baseline and for the final geometry. As seen, the cost function, which reflects the distribution of mass in the channels, has been

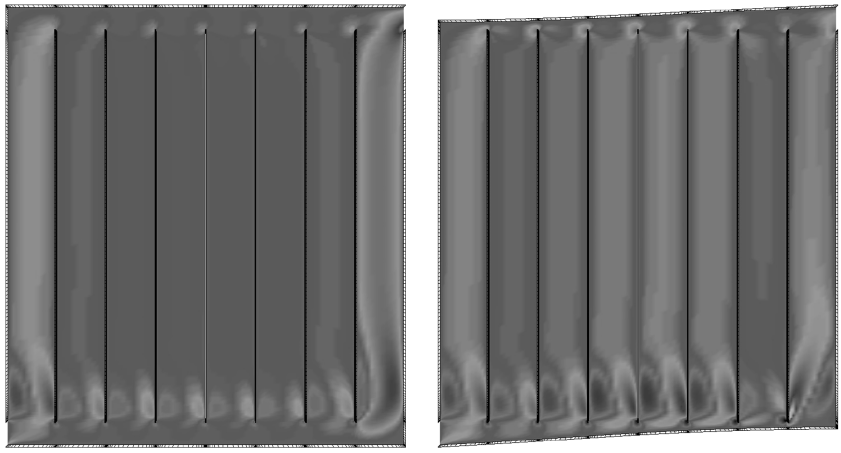

a) Initial geometry for manifold **b) Modified geometry for manifold**

Fig. 17 Design for distributing fluid evenly among channels in a manifold.

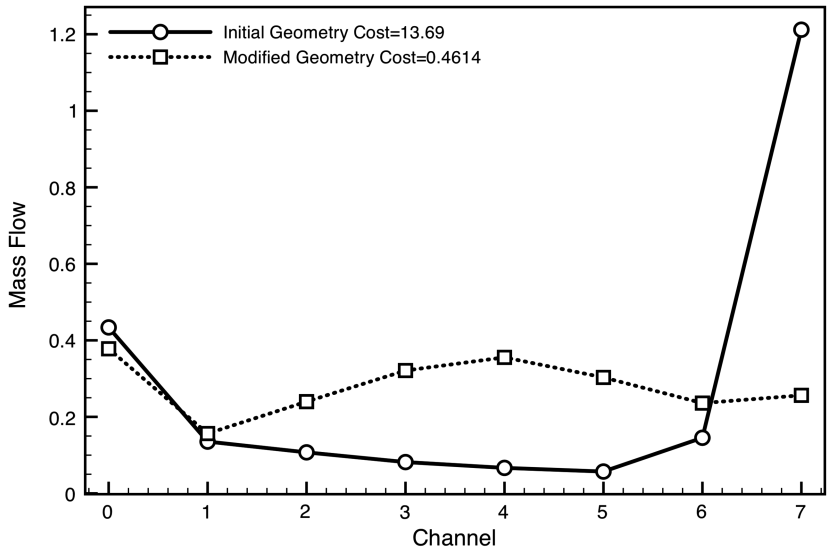

Fig. 18 Distribution of mass flow among channels.

reduced by almost a factor of 30. Furthermore, a much more even distribution of fluid is obtained across the channels.

IV. Conclusions

A new procedure has been developed to parameterize geometries for use in design optimization. The technique may be used in multidisciplinary applications and provides a viable alternative to free-form deformation. With the present method, the design parameters are typically distributed on the surface of a volume and not within the interior. As a consequence, the number of design variables may be increased without an associated cubic increase in the total number of design variables, as occurs with free-form deformation. Further, in the approach described here, the control grid is held fixed during the entire design cycle, thereby eliminating the risk of it folding on itself. In contrast, when using free-form deformation, the perturbations at each point of the NURBS or B-spline volume obtained during the course of an optimization can cause overlapping of the points in the NURBS volume itself. Neither the present approach nor free-form deformation guarantees that the geometry itself will not cross without placing constraints on the design variables. Finally, the technique described here provides for arbitrary-shaped control grids, because it does not require an underlying structured indexing scheme associated with free-form deformation.

Although the present approach provides an alternative to free-form deformation and has several advantages, there are two disadvantages to the current method when compared with free-form deformation. First, the free-form deformation can be readily used for modifying geometries over subsections of a geometry without risking the development of nonsmooth second derivatives at the juncture between the fixed and variable sections. Modifications are under development for the present method to provide similar capability. The second disadvantage of the current method is that approximate numerical solutions to partial differential equations are needed for each design variable. In practice, this is not a major disadvantage because the solutions do not have to be well converged and are only required at the beginning of the overall design process.

The method has been implemented in both two and three dimensions, and exemplary designs have been demonstrated.

Acknowledgments

This work has been sponsored by the Tennessee Higher Education Commission Center of Excellence for Applied Computational Science and Engineering under the direction of Henry McDonald. This support is gratefully acknowledged. The authors would also like to thank Jamshid Samareh for useful discussions on parameterization methods.

References

[1] Hicks, R. M., and Henne, P. A., "Wing Design by Numerical Optimization," *Journal of Aircraft*, Vol. 15, No. 7, 1978, pp. 407–412. doi:10.2514/3.58379

[2] Angrand, F., "Optimum Design for Potential Flows," *International Journal for Numerical Methods in Fluids*, Vol. 3, 1983, pp. 265–282. doi:10.1002/fld.1650030306

[3] Jameson, A., "Aerodynamic Design via Control Theory," *Journal of Scientific Computing*, Vol. 3, 1988, pp. 233–260. doi:10.1007/BF01061285

[4] Drela, M., "Design and Optimization Method for Multi-Element Airfoils," AIAA Paper 93-0969, Feb. 1993.

[5] Burgreen, G. W., and Baysal, O., "Three-Dimensional Aerodynamic Shape Optimization of Wings Using Sensitivity Analysis," AIAA Paper 94-0094, Jan. 1994.

[6] Jameson, A., Alonso, J. J., Reuther, J., Martinelli, L., and Vassberg, J. C., "Aerodynamic Shape Optimization Techniques Based on Control Theory," AIAA Paper 98-2538, 1998.

[7] Anderson, W. K., and Venkatakrishnan, V., "Aerodynamic Design Optimization on Unstructured Grids with a Continuous Adjoint Formulation," *Computers and Fluids*, Vol. 28, Nos. 4–5, 1999, pp. 443–480. doi:10.1016/S0045-7930(98)00041-3

[8] Anderson, W. K., and Bonhaus, D. L., "Airfoil Design on Unstructured Grids for Turbulent Flows," *AIAA Journal*, Vol. 37, No. 2, 1999, pp. 185–191. doi:10.2514/2.712

[9] Nielsen, E. J., and Anderson, W. K., "Aerodynamic Design Optimization on Unstructured Meshes Using the Navier–Stokes Equations," *AIAA Journal*, Vol. 37, No. 11, 1999, pp. 1411–1419. doi:10.2514/2.640

[10] Burdyshaw, C. E., "Quasi 3D Multi-Stage Turbomachinery Pre-Optimizer," M.S. Thesis, Mississippi State Univ., Mississippi State, MS, 2001.

[11] Nielsen, E. J., and Anderson, W. K., "Recent Improvements in Aerodynamic Optimization on Unstructured Meshes," *AIAA Journal*, Vol. 40, No. 6, 2002, pp. 1155–1163. doi:10.2514/2.1765

[12] Kim, H., Koc, S., and Nakahashi, K., "Surface Modification Method for Aerodynamic Design Optimization," *AIAA Journal*, Vol. 43, No. 4, April 2005, pp. 727–740. doi:10.2514/1.11181

[13] Fudge, D. M., and Zingg, D. W., "A CAD-Free and a CAD-Based Geometry Control System for Aerodynamic Shape Optimization," AIAA Paper 2005-0451, 2005.

[14] Samareh, J. A., "A Novel Shape Parameterization Approach," NASA TM/TM-1999-209116, May 1999.

[15] Samareh, J. A., "A Survey of Shape Parameterization Techniques for High-Fidelity Multidisciplinary Shape Optimization," *AIAA Journal*, Vol. 39, May 2001, pp. 877–884. doi:10.2514/2.1391

[16] Smith, R. E., Bloor, M. L. G., Wilson, M. J., and Thomas, A. M., "Rapid Airplane Parametric Input Design," AIAA Paper 95-1687, 1995.

[17] Leiva, J. P., and Watson, B. C., "Automatic Generation of Basis Vectors for Shape Optimization in the GENESIS program," AIAA Paper 1998-4852, Sept. 1998.

[18] Samareh, J. A., "Multidisciplinary Aerodynamic-Structural Shape Optimization Using Deformation (MASSOUD)," AIAA Paper 2000-4911, 2000.

[19] Samareh, J. A., "Aerodynamic Shape Optimization Based on Free-Form Deformation," AIAA Paper 2004-4630, 2004.

[20] Sarakinos, S. S., Amoiralis, E., and Nikolos, I. K., "Exploring Freeform Deformation Capabilities in Aerodynamic Shape Parameterization," *International Conference on Computer as a Tool*, 2005, pp. 535–538.doi:10.1109/EURCON.2005.1629983

[21] Venkatakrishnan, V., and Mavriplis, D. J., "Implicit Method for the Computation of Unsteady Flows on Unstructured Grids," *Journal of Computational Physics*, Vol. 127, 1996, pp. 380–397. doi:10.1006/jcph.1996.0182

[22] Yang, Z., and Mavriplis, D. J., "Mesh Deformation Strategy Optimized by the Adjoint Method on Unstructured Meshes," *AIAA Journal*, Vol. 45, No. 12, 2007, pp. 2885–2896. doi:10.2514/1.30592

[23] Truong, A., Oldfield, C. A., and Zingg, D. W., "Mesh Movement for a Discrete-Adjoint Newton–Krylov Algorithm for Aerodynamic Optimization," *AIAA Journal*, Vol. 46, No. 7, July 2008, pp. 1695–1704. doi:10.2514/1.33836

[24] Fox, P. A., Hall, A. D., and Schryer, N. L., "The PORT Mathematical Subroutine Library," *Transactions on Mathematical Software*, Vol. 4, No. 2, June 1978, pp. 104–126.doi:10.1145/355780.355783

[25] Pirzadeh, S., "Structured Background Grids for Generation of Unstructured Grids by Advancing-Front Method," *AIAA Journal*, Vol. 31, No. 2, 1993, pp. 257–265. doi:10.2514/3.11662

[26] Anderson, W. K., and Bonhaus, D. L., "An Implicit Upwind Algorithm for Computing Turbulent Flows on Unstructured Grids," *Computers and Fluids*, Vol. 23, No. 1, 1994, pp. 1–21. doi:10.1016/0045-7930(94)90023-X

[27] Anderson, W. K., Newman, J. C., Whitfield, D. L., and Nielsen, E. J., "Sensitivity Analysis for the Navier–Stokes Equations on Unstructured Meshes Using Complex Variables," *AIAA Journal*, Vol. 39, No. 1, 2001, pp. 56–63. doi:10.2514/2.1270

[28] Newman, J. C., Anderson, W. K., and Whitfield, D. L., "Multidisciplinary Sensitivity Derivatives Using Complex Variables," Mississippi State Univ. MSSU-COE-ERC-98-08, 1998.

[29] Newman, J. C., Anderson, W. K., and Whitfield, D. L., "A Step-Size Independent Approach to Multidisciplinary Sensitivity Analysis," *Journal of Aircraft*, Vol. 40, No. 3, 2003, pp. 566–573. doi:10.2514/2.3131

[30] Cook, P. H., McDonald, M. A., and Firmin, M. C. P., "Aerofoil RAE

2822—Pressure Distributions, and Boundary Layer and Wake Measurements," *Experimental Data Base for Computer Program Assessment*, AGARD Rept. AR 138, 1979.

[31] Whitcomb, R. T., and Clark, L. R., "An Airfoil Shape for Efficient Flight at Supercritical Mach Numbers," NASA TM X-1109, 1965.

[32] Sreenivas, K., Hyams, D. G., Nichols, D. S., Mitchell, B., Taylor, L. K., Briley, W. R., and Whitfield, D. L., "Development of an Unstructured Parallel Flow Solver for Arbitrary Mach Numbers," AIAA Paper 2005-0325, Jan. 2005.

[33] Sreenivas, K., Taylor, L., and Briley, R., "A Global Preconditioner for Viscous Flow Simulations at All Mach Numbers," AIAA Paper 2006-3852, June 2006.

[34] Burdyshaw, C. E., and Anderson, W. K., "A General and Extensible Unstructured Mesh Adjoint Method," *Journal of Aerospace Computing, Information, and Communication*, Vol. 2, No. 10, 2005, pp. 401–413.
doi:10.2514/1.15932

[35] Burdyshaw, C. E., "Achieving Automatic Concurrency Between Computational Field Solvers and Adjoint Sensitivity Codes," Ph.D. Thesis, Univ. of Tennessee, Chattanooga, TN, May 2006.

E. Livne
Associate Editor